Field-induced optical absorption in two-dimensional lattices

2006 J. Phys.: Condens. Matter 18 6193

(http://iopscience.iop.org/0953-8984/18/27/003)

INSTITUTE OF PHYSICS PUBLISHING JOURNAL OF PHYSICS: CONDENSED MATTER

J. Phys.: Condens. Matter **18** (2006) 6193–6200 doi:10.1088/0953-8984/18/27/003

Field-induced optical absorption in two-dimensional lattices

Y Zhao[1], **Y F Wang**[1] **and C D Gong**[2,1]

[1] National Laboratory of Solid State Microstructures and Department of Physics, Nanjing University, Nanjing 210093, People's Republic of China
[2] Chinese Center of Advanced Science and Technology (World Laboratory), PO Box 8730, Beijing 100080, People's Republic of China

E-mail: yfwang_nju@hotmail.com

Received 26 April 2006
Published 23 June 2006
Online at stacks.iop.org/JPhysCM/18/6193

Abstract

We present a detailed analysis of the field-induced optical absorption (FIOA) in square and triangular lattices based on the tight-binding lattice-electron model with hopping integrals modulated by the staggered magnetic flux (SMF). The SMF generates a two-sublattice system with two branches of energy band in both cases, and the inter-band optical transition dominates the absorption spectrum. The dependence of the main absorption peak (MAP) frequency and the absorption spectra weight on the flux parameter δ and chemical potential μ are discussed in detail.

(Some figures in this article are in colour only in the electronic version)

1. Introduction

The orbital dynamics of two-dimensional (2D) lattice electrons coupled to a uniform magnetic field has shown extremely rich and interesting behaviour (e.g. the well-known Hofstadter's butterfly-like spectrum [1]). This system is similar to the perfect network of Aharonov–Bohm (AB) rings in some aspects. An electron hopping from one site to its nearest neighbours suffers a phase shift due to the AB effect. Because of the phase shift, the quantum interference effect occurs and will be reflected in the behaviour of physical quantities which become periodic functions of the magnetic flux. Compared with a uniform magnetic field, various spatially modulated magnetic fields can lead to additional interesting physics, e.g. the interesting transmission behaviour in quasi-1D (one-dimensional) chains [2, 3], the field-induced metal–insulator transition and d-wave pseudogap opened on the Fermi surface in 2D square lattices [4], the generic breakdown effect on the symmetries, and the fractal property of Hofstadter's spectrum [5].

It is now experimentally possible to construct and detect the inhomogeneous field on the deep sub-micron scale [6, 7]. Also, recently, adopting a superconductor/ferromagnet hybrid

system consisting of a superconducting wire network and an array of mesoscopic ferromagnets, magnetic fields with staggered configurations have been realized experimentally [8–10]. Thus the properties of quantum systems [2–5] based on quasi-1D or 2D lattices under spatially modulated magnetic fields are very foreseeable in future experiments.

In connection with the above noninteracting electron systems, an interacting spin or electron model in the square lattice with appropriate parameters, after taking a particular mean-field decoupling, can be simplified to a nearly free electronic system under a $\sqrt{2}\times\sqrt{2}$ staggered magnetic flux [11–13]. Also, a phase with a $1\times\sqrt{3}$ staggered magnetic flux has been considered as the mean-field ansatz [14] for the Heisenberg model in the triangular lattice. In these cases, the corresponding magnetic flux is related to the minimum energy, and is not a free variable parameter.

Although the energy spectral and transport properties of lattice electrons under spatially modulated magnetic fields have been investigated in detail [2–5, 15–17, 10, 18], the corresponding optical properties of such systems have rarely been explored. It is well known that the ability of optical absorption in the nearly free particle system depends on its imperfections or deviations from homogeneity [19]. For example, the inhomogeneity induced by the crystalline potential leads to optical absorption through interband transitions in metal, and the deviation from the periodic crystalline potential due to lattice vibration generates the phonon-induced optical absorption. Obviously, an external staggered magnetic flux (SMF) will create a special type of inhomogeneity in lattice electron systems, and hence should lead to SMF-induced optical absorption.

In this paper, we investigate the optical absorption of 2D systems with staggered magnetic flux (SMF). We first calculate the SMF-induced modification to the electronic dispersion based on the tight-binding model, with hopping integrals modulated by the magnetic flux. The obtained energy bands depend on the strength and periodicity of the SMF. As a result of interaction between the external electromagnetic wave and the electrons with SMF-dependent dispersion, the optical absorption spectrum will show different behaviour from that in the absence of SMF. The optical absorption spectrum can be controlled by adjusting the electron density and the strength of SMF.

The paper is organized as follows. In section 2, the approach of calculating field-induced optical absorption (FIOA) with the standard Kubo formula is presented. In the following two sections, we apply the framework to the square and triangular lattices, respectively. A summary is given in the last section.

2. The approach

In a 2D system, based on the tight-binding model with SMF, the hopping integral t_{ij} of electrons from lattice point i to lattice point j is modified by a phase factor because electron hopping from one site to its nearest neighbours suffers a phase shift due to the Aharonov–Bohm (AB) effect. The corresponding Hamiltonian H can be diagonalized in k-space through Fourier transformation, which leads to an SMF-dependent multi-band energy spectrum in general.

To study the optical transitions, we introduce the interaction of electrons with an external electromagnetic (EM) field propagating along the 2D plane. The vector potential of the light, $\vec{A}$, is also assumed in the 2D plane; its wavelength is much longer than the lattice constant a. Then the complex conductivity is given by the standard Kubo formula [19]:

$$\sigma(\omega) = \frac{e^2\hbar}{\mathrm{i}\omega\pi N}\sum_{m,n}|\langle n|\overrightarrow{j}|m\rangle|^2\frac{f(E_m)-f(E_n)}{\hbar\omega^+ - E_m + E_n} \tag{1}$$

where E_n is the corresponding eigenvalue of the eigenstate $|n\rangle$, N is the number of sites, and

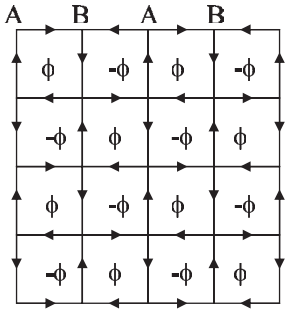

Figure 1. A 2D square lattice with plaquette threaded by alternative flux ϕ and $-\phi$. Electrons hopping along (against) the arrows suffer a phase shift of $\delta/4$ ($-\delta/4$), where $\delta = 2\pi\phi/\phi_0$.

$\omega^+ = \omega + \mathrm{i}0^+$. The current operator $\overrightarrow{j} = \sum_\tau j_\tau \vec{e}_\tau$, and the component in the τ direction is defined as $j_\tau = \mathrm{i}\sum_i [c^\dagger_{i+\tau} c_i \exp(\mathrm{i}\phi_{i+\tau,i}) - c^\dagger_i c_{i+\tau} \exp(-\mathrm{i}\phi_{i+\tau,i})]$. The real part of (1) gives the optical absorption.

3. FIOA in the 2D square lattice

Consider the two-dimensional square lattice with the SMF [4, 20] as shown in figure 1. From the topology of the system, we can conclude that it is a two-sublattice system: sublattice A and sublattice B. Let $\alpha^\dagger$ (or $\beta^\dagger$) denote the creation operator in sublattice A (or B). The Hamiltonian can be written in k-space as

$$H = -2t \sum_{k\sigma} (\gamma_k \alpha^\dagger_{k\sigma} \beta_{k\sigma} + \mathrm{H.c.}), \tag{2}$$

where $\gamma_k = \exp(\mathrm{i}\delta/4)\cos k_x a + \exp(-\mathrm{i}\delta/4)\cos k_y a$, $\delta = 2\pi\phi/\phi_0$ ($\phi_0 = hc/e$ is the flux quantum) is the flux parameter to represent the strength of the SMF, and t is the hopping integral in the absence of SMF. Through direct diagonalization, we have two branches of energy spectrum, $E_{1k} = 2t|\gamma_k|$ and $E_{2k} = -2t|\gamma_k|$, and the corresponding wave functions $|1\rangle = (1/\sqrt{2})(1, |\gamma_k|/\gamma_k)^{\mathrm{T}}$ and $|2\rangle = (1/\sqrt{2})(-1, |\gamma_k|/\gamma_k)^{\mathrm{T}}$. In the following expressions, we denote $\gamma_k/|\gamma_k| \equiv \exp(\mathrm{i}\theta_k)$, and have $\tan\theta_k = [\cos k_x a - \cos k_y a]/[\cos k_x a + \cos k_y a]\tan(\delta/4)$.

The current operator $\overrightarrow{j}$ can also be written in k-space as a 2×2 matrix like the Hamiltonian. Then we calculate the vertex functions, $|\langle 1|\overrightarrow{j}|1\rangle|^2$ ($= |\langle 2|\overrightarrow{j}|2\rangle|^2$) and $|\langle 1|\overrightarrow{j}|2\rangle|^2$ ($= |\langle 2|\overrightarrow{j}|1\rangle|^2$), insert them into (1), and obtain the optical absorption

$$\begin{aligned}\mathrm{Re}\,[\sigma(\omega)] = \sum_k (\sin^2 k_x a + \sin^2 k_y a) \Bigg\{ &\left[2 + 2\cos\left(\frac{\delta}{2} + 2\theta_k\right)\right]\left[-\frac{\partial n_{1k}}{\partial E_{1k}} - \frac{\partial n_{2k}}{\partial E_{2k}}\right]\delta(\omega) \\ &+ \left[2 - 2\cos\left(\frac{\delta}{2} + 2\theta_k\right)\right] \frac{\sinh(2\beta t|\gamma_k|)}{\cosh(2\beta t|\gamma_k|) + \cosh(\beta\mu)} \frac{1}{\omega}\delta\left(\omega - 4t|\gamma_k|\right)\Bigg\}\end{aligned} \tag{3}$$

where $n_{1k} = 1/\{\exp[\beta(E_{1k} - \mu)] + 1\}$ and $n_{2k} = 1/\{\exp[\beta(E_{2k} - \mu)] + 1\}$.

We introduce phenomenological relaxation time τ to include effects of phonons and disorder. Then ω^+ in (1) should be replaced by $\omega + \mathrm{i}/\tau$ ($1/\tau$ is often called the damping parameter). The corresponding replacements $\delta(\omega) \to \tau/(1 + \omega^2\tau^2)$ and $1/\omega \to \omega\tau^2/(1 + \omega^2\tau^2)$ will be adopted in the subsequent calculations of (3).

From (3) we can see that the optical absorption spectrum is composed of the intra-band and inter-band transitions within the two branches of the energy bands. The spectra distribution depends on the flux parameter δ and the chemical potential μ (which is related to the electron

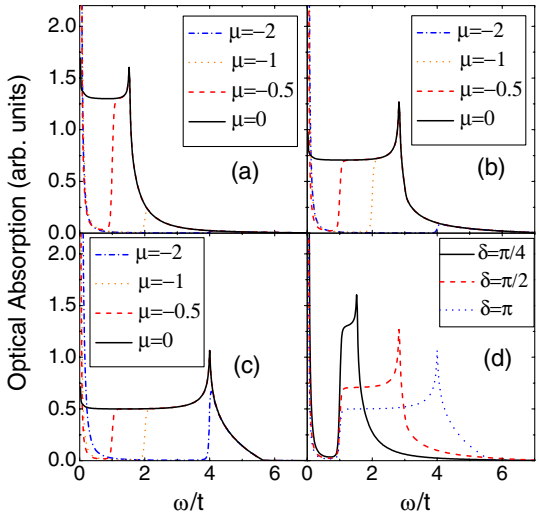

Figure 2. Square lattice: FIOA (in arbitrary units) versus frequency (in units of t) for various flux parameters δ and chemical potentials μ (in units of t). The damping parameter $1/\tau = 0.01t$. (a) $\delta = \pi/4$; (b) $\delta = \pi/2$; (c) $\delta = \pi$; (d) $\mu = -0.5$.

filling factor ν through the integration of the density of states (DOS), namely $\nu = \int_{\epsilon_{\min}}^{\mu} D(\epsilon)\,\mathrm{d}\epsilon$; here $\epsilon_{\min}$ is the lower limit of the DOS function). We can also see that the optical absorption rate is not only related to the DOS of the upper and lower bands, but is also determined by the strong field and momentum dependence of the two vertex functions $|\langle 1|\overrightarrow{j}|1\rangle|^2$ and $|\langle 1|\overrightarrow{j}|2\rangle|^2$.

It should be noted that, due to the period and symmetry of the DOS [4], the corresponding absorption spectrum is a periodic function of δ with a period of π. For $\delta = 0$ (no magnetic field), we have only one energy band, and our calculation shows that the absorption spectra weight is concentrated in the Drude weight at low frequency.

In figures 2(a)–(c), the absorption spectra are plotted for $\delta = \pi/4$, $\pi/2$ and π with a different chemical potential μ. Here the optical absorption is also an even function of μ due to the symmetry of the DOS. Hence, we consider the case $\mu \leqslant 0$ only, and concentrate our attention on the case $\delta = \pi/4$. When $\mu = -2$ (in units of t), there is a remnant Drude peak at low frequency, a low and broad hump at high frequency, and no absorption spectrum in the intermediate frequency region. When μ changes from -2 to -0.5, the hump at high frequency grows and shifts to lower frequency, eating up the intermediate gap in the spectrum gradually, and becomes a big and sharp peak at $\mu = -0.5$. While at $\mu = 0$ (the half-filled case), the Drude peak at low frequency disappears and is covered by the left wing of the main absorption peak (MAP). The absorption spectrum weight decreases upon an increase in $|\mu|$. This is due to the phase space available for electron transition becoming smaller.

We also plot the variations in optical spectrum with δ at a given $\mu = -0.5$ in figure 2(d). When the flux parameter δ changes from $\pi/4$ to π, the position of the absorption peak and spectra weight are transferred to the higher frequency region, while the height of the peak is lowered.

In order to consider the evolution of the MAP frequency ($\Omega_{\mathtt{MAP}}$) in the absorption spectra with the flux parameter δ, we plot the contour plots of FIOA in the δ–ω parameter space (figure 3). From the darker lines in figure 3, it is easy to verify that $\Omega_{\mathtt{MAP}}(\delta) = 4t|\sin\frac{\delta}{2}|$ except for the low-frequency cutoff, which is determined by the chemical potential μ. We note that $4t|\sin\frac{\delta}{2}|$ is the frequency difference between two Van Hove singularities (VHS) in the DOS [4].

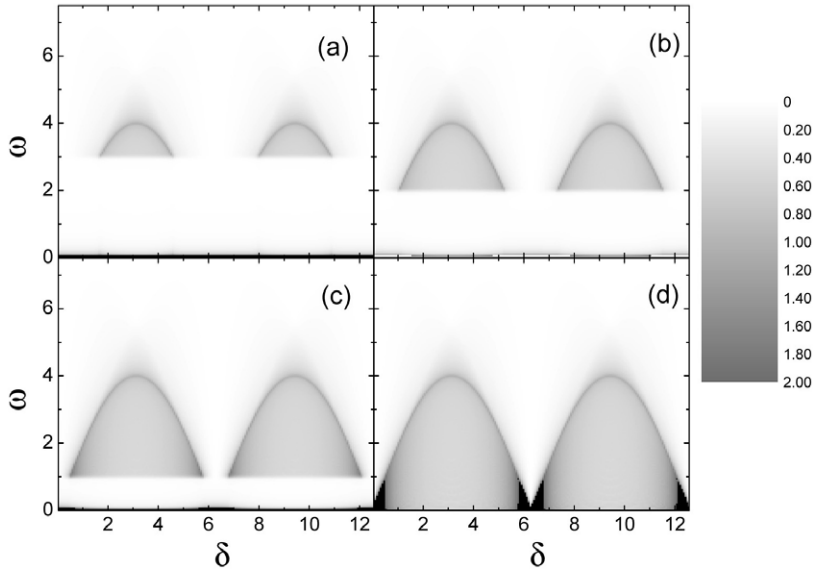

Figure 3. Square lattice: the contour plots of FIOA (in arbitrary units) in the δ–ω parameter space for different chemical potentials μ: (a) $\mu = -1.5$; (b) $\mu = -1$; (c) $\mu = -0.5$; (d) $\mu = 0$. μ and ω are in units of t, and the damping parameter $1/\tau = 0.01t$.

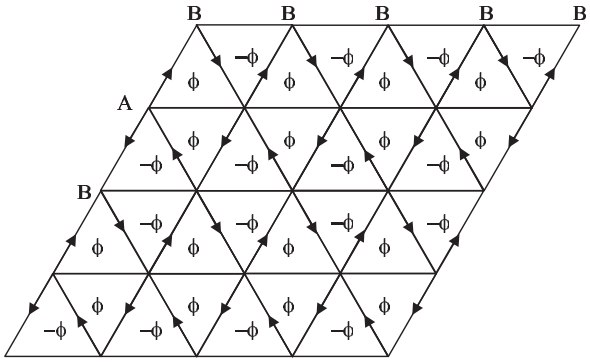

Figure 4. A 2D triangular lattice with plaquette threaded by alternative flux ϕ and $-\phi$. Electrons hopping along (against) the arrows suffer a phase shift of $\delta/2$ $(-\delta/2)$, where $\delta = 2\pi\phi/\phi_0$.

For small $|\mu|$ and $|\mathtt{mod}(\delta, 2\pi) - \pi|$ (e.g. the case $\mu = -0.5$ and $\delta = \pi$ in figure 2(c)), there are two VHSs (in the two bands), one below the Fermi level and another above it, hence there is a MAP in absorption spectra. While for large $|\mu|$ or large $|\mathtt{mod}(\delta, 2\pi) - \pi|$ (e.g. the case $\mu = -2$ and $\delta = \pi/4$ in figure 2(a)), both VHSs are above or below the Fermi level, there is only a hump (no MAP).

4. FIOA in the 2D triangular lattice

Consider the two-dimensional triangular system with the SMF [18] as shown in figure 4. From the topology of the system, we can see that it is a two-sublattice system: sublattice A and sublattice B. Let $\alpha^\dagger$ (or $\beta^\dagger$) denote the creation operator in sublattice A (or B). The Hamiltonian

in k-space is

$$H = -2t \sum_{k\sigma} \left(\alpha^{\dagger}_{k\sigma}, \beta^{\dagger}_{k\sigma}\right) \begin{pmatrix} u_k & v_k^* \\ v_k & u_k \end{pmatrix} \begin{pmatrix} \alpha_{k\sigma} \\ \beta_{k\sigma} \end{pmatrix}, \tag{4}$$

where $u_k = \cos k_x a$, and $v_k = \mathrm{e}^{\mathrm{i}\delta/2} \cos(\frac{1}{2}k_x a + \frac{\sqrt{3}}{2}k_y a) + \mathrm{e}^{-\mathrm{i}\delta/2} \cos(\frac{1}{2}k_x a - \frac{\sqrt{3}}{2}k_y a)$.

After direct diagonalization of the Hamiltonian, we also have two branches of energy spectrum $E_1(k) = -2tu_k + 2t|v_k|$ and $E_2(k) = -2tu_k - 2t|v_k|$ and the corresponding wave functions $|1\rangle = (1/\sqrt{2})(1, |v_k|/v_k)^{\mathrm{T}}$ and $|2\rangle = (1/\sqrt{2})(-1, |v_k|/v_k)^{\mathrm{T}}$. In the following expressions, we denote $v_k/|v_k| \equiv \exp(\mathrm{i}\theta_k)$ and have $\tan\theta_k = -\tan\frac{1}{2}k_x a \tan\frac{\sqrt{3}}{2}k_y a \tan\delta/2$.

The optical absorption is given by

$$\begin{aligned} \mathrm{Re}[\sigma(\omega)] = \sum_k \Bigg\{ & |\langle 1|\overrightarrow{j}|1\rangle|^2 \left[-\frac{\partial n_{1k}}{\partial E_{1k}} - \frac{\partial n_{2k}}{\partial E_{2k}}\right] \delta(\omega) \\ & + |\langle 1|\overrightarrow{j}|2\rangle|^2 \frac{\sinh(2\beta t|v_k|)}{\cosh(2\beta t|u_k| + \beta\mu) + \cosh(2\beta t|v_k|)} \frac{1}{\omega} \delta(\omega - 4t|v_k|) \Bigg\} \end{aligned} \tag{5}$$

where $n_{1k} = 1/\{\exp[\beta(E_{1k} - \mu)] + 1\}$, $n_{2k} = 1/\{\exp[\beta(E_{2k} - \mu)] + 1\}$, and the vertex functions are:

$$\begin{aligned} |\langle 1|\overrightarrow{j}|1\rangle|^2 = {} & 16 \sin^2 \frac{1}{2}k_x a \cos^2 \frac{\sqrt{3}}{2}k_y a \cos^2 \frac{\delta}{2} \cos^2\theta_k \\ & + 16 \cos^2 \frac{1}{2}k_x a \sin^2 \frac{\sqrt{3}}{2}k_y a \sin^2 \frac{\delta}{2} \sin^2\theta_k \\ & + 8 \sin k_x a \left(\sin \frac{1}{2}k_x a \cos \frac{\sqrt{3}}{2}k_y a \cos \frac{\delta}{2} \cos\theta_k \right. \\ & \left. - \cos \frac{1}{2}k_x a \sin \frac{\sqrt{3}}{2}k_y a \sin \frac{\delta}{2} \sin\theta_k \right) \\ & + 4 \sin^2 k_x a + \sin k_x a \sin\sqrt{3}k_y a \sin\delta \sin 2\theta_k \\ |\langle 1|\overrightarrow{j}|2\rangle|^2 = {} & 16 \sin^2 \frac{1}{2}k_x a \cos^2 \frac{\sqrt{3}}{2}k_y a \cos^2 \frac{\delta}{2} \sin^2\theta_k \\ & + 16 \cos^2 \frac{1}{2}k_x a \sin^2 \frac{\sqrt{3}}{2}k_y a \sin^2 \frac{\delta}{2} \cos^2\theta_k \\ & - \sin k_x a \sin\sqrt{3}k_y a \sin\delta \sin 2\theta_k . \end{aligned}$$

As for the square lattice, the phenomenological relaxation time τ is also introduced to account for the effects of phonons and disorder. For $\delta = \pi/8$, the dependence of the absorption spectrum on the chemical potential μ (i.e. the change in doping density) is shown in figure 5(a). We note that, when $\mu = 0$ (the half-filled case), the absorption shows a low and broad hump. When μ changes from 0 to -2 then -3 (hole doping case), the hump disappears gradually. When μ changes from 0 to 1 then to 2 (electron doping case), the hump increases and gradually forms a peak.

When the flux parameter increases to $\delta = \pi/4$ (figure 5(b)), the absorption peak becomes prominent and its location shifts to the neighbourhood of $\omega = 3$ when μ changes from 0 to 2. For $\mu = 3$, the peak is replaced by a hump.

As δ increases further to $\delta = \pi/2$ (figure 5(c)), the peak in the $\mu = 0$ case becomes more prominent. The absorption spectra for μ and $-\mu$ are the same due to the fact that the DOS [18] is symmetric about energy. In heavily doped regions, for both hole and electron doping ($|\mu| > 2.5$), the peak is replaced by a hump.

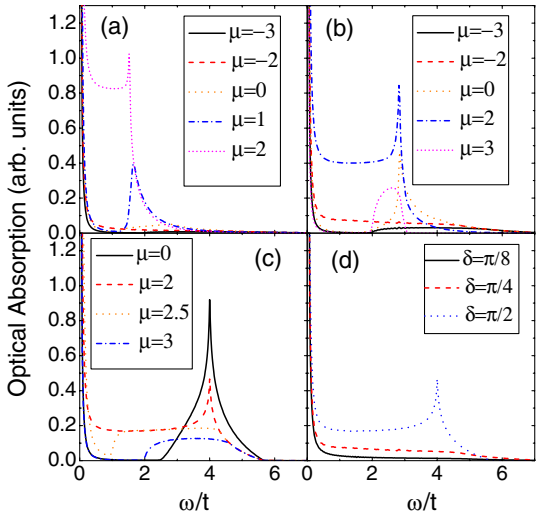

Figure 5. Triangular lattice: FIOA (arbitrary units) versus frequency (in units of t) for various flux parameters δ and chemical potentials μ (in units of t). The damping parameter $1/\tau = 0.01t$. (a) $\delta = \pi/8$; (b) $\delta = \pi/4$; (c) $\delta = \pi/2$; (d) $\mu = -2$.

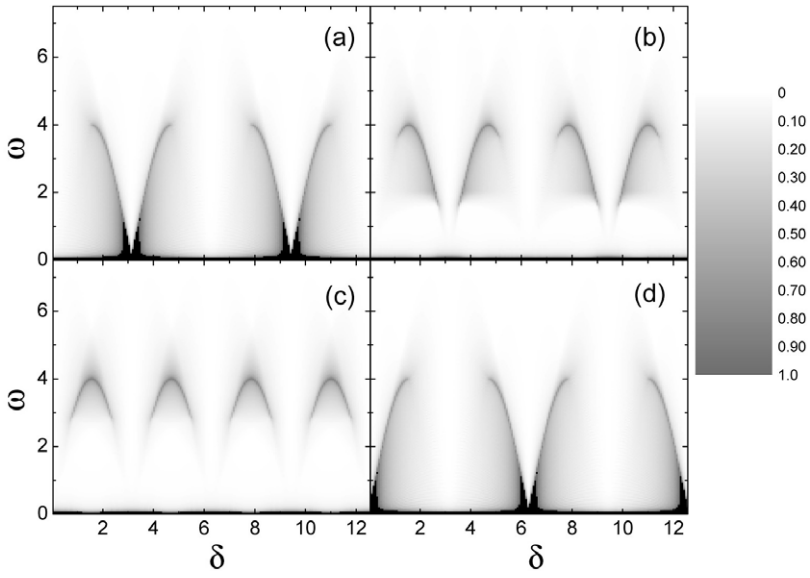

Figure 6. Triangular lattice: the contour plots of FIOA (arbitrary units) in the δ–ω parameter space for different chemical potential μ: (a) $\mu = -2$; (b) $\mu = -1$; (c) $\mu = 0$; (d) $\mu = 2$. μ and ω are in units of t, and the damping parameter $1/\tau = 0.01t$.

We also plot the variations of the optical spectrum with δ at a given $\mu = -2.0$ in figure 5(d). When the flux parameter δ changes from $\pi/8$ to $\pi/2$, the broad absorption tail evolves into a peak and the spectra weights are shifted to the lower frequency region.

The contour plots of FIOA in the δ–ω parameter space are plotted in figure 6. From the darker lines, we can see that the MAP frequencies Ω_{MAP} satisfy $\Omega_{\mathrm{MAP}}(\delta) = 4t|\sin\delta|$ in general.

Also, the asymmetric cutoffs are related to the multi-VHS structure of the DOS [18]. Similarly to the square lattice, for small $|\mu|$ and small $|\mathtt{mod}(\delta, \pi)-\pi/2|$ (e.g. the case $\mu = 0$ and $\delta = \pi/2$ in figure 5(c)), there is MAP, otherwise (e.g. the case $\mu = 3$ and $\delta = \pi/4$ in figure 5(b)) a hump will replace MAP. The reasons are also similar to the square lattice.

The scheme that we have presented here can also be used to calculate the optical properties of any 2D lattices under any kind of modulated magnetic field. The optical absorption studies may provide an approach to detect whether the breaking of time-reversal symmetry happens or not in a real material, because it will lead to the appearance of SMF or not.

5. Summary

In this paper we have presented a detailed analysis of field-induced optical absorption for the square and triangular lattices based on the tight-binding model with the hopping integrals modulated by the magnetic flux. The applied staggered magnetic field generates a two-sublattice system with two branches of energy bands. We find that the optical absorption spectrum comes mainly from the interband transition, while the intraband transitions only contribute to the optical absorption at very low frequency with a conventional Drude peak. Also, the spectrum is not only related to the DOS of the upper and lower bands, but is also determined by the strong field and momentum dependence of the vertex functions. The strong SMF and momentum dependence of the MAP frequency and the absorption spectral weight on the flux parameter δ and chemical potential μ are also discussed.

Accordingly, through adjusting the two parameters δ (the SMF) and μ (or the corresponding electron filling factor), we can control the structure, peak location and weight of the field-induced absorption spectrum.

Acknowledgment

This work is supported by the Chinese National Natural Science Foundation.

References

[1] Hofstadter D R 1976 *Phys. Rev.* B **14** 2239
[2] Pan Z W, Gong C D, Lung M K and Lin H Q 1999 *Phys. Rev.* E **59** 6010
[3] Lung M K, Lin H Q, Pan Z W and Gong C D 2000 *J. Appl. Phys.* **87** 30
[4] An J, Gong C D and Lin H Q 2001 *Phys. Rev.* B **63** 174434
[5] Oh G Y 1999 *Phys. Rev.* B **60** 1939
[6] Cowburn R P, Koltsov D K, Adeyeye A O and Welland M E 1998 *Appl. Phys. Lett.* **73** 3947
[7] Cowburn R P, Koltsov D K, Adeyeye A O and Welland M E 2000 *J. Appl. Phys.* **87** 7067
[8] Ito S, Ando M, Katsumoto S and Iye Y 1999 *J. Phys. Soc. Japan* **68** 3158
[9] Ando M, Ito S, Katsumoto S and Iye Y 1999 *J. Phys. Soc. Japan* **68** 3462
[10] Iye Y, Kuramochi E, Hara M, Endo A and Katsumoto S 2004 *Phys. Rev.* B **70** 144524
[11] Affleck I and Marston J B 1988 *Phys. Rev.* B **37** R3774
[12] Marston J B and Affleck I 1989 *Phys. Rev.* B **39** 11538
[13] Nayak C 2000 *Phys. Rev.* B **62** 4880
[14] Lee T K and Feng S P 1990 *Phys. Rev.* B **41** 11110
[15] Gumbs G, Miessein D and Huang D 1995 *Phys. Rev.* B **52** 14755
[16] Oh G Y and Lee M H 1996 *Phys. Rev.* B **53** 1225
[17] Shi Q W and Szeto K Y 1997 *Phys. Rev.* B **56** 9251
[18] Wang Y F, Gong C D and Zhu S Y 2005 *Europhys. Lett.* **69** 404
[19] Mahan G D 1990 *Many-Particle Physics* (New York: Plenum)
[20] Harris A B, Lubensky T C and Mele E J 1989 *Phys. Rev.* B **40** R2631